Taylor & Francis
Taylor & Francis Group

Check for updates

Effective input velocity and depth for deep and shallow sites for site response analysis

Ketan Bajaj and P Anbazhagan

Department of Civil Engineering, Indian Institute of Science, Bangalore, India

ABSTRACT

Ground motion input layer depth and V_s are crucial parameters in computing representative surface amplification factor, especially for deep deposits where bedrock depth is unknown. For many soil sites, seismic bedrock depth is unknown and randomly assigning the input motion to any layer may result in bias response. The aim of this study is to understand the effect of input layer velocity or depth on surface response parameters. Further determining the appropriate layer for giving the input ground motion for reliable estimation of response parameters by carrying out detailed site-response analysis. For the analysis, surface and bedrock ground motion recordings from KiK-Net downhole are used. Total stress nonlinear site-response analysis has been carried out by varying the velocity and depth to input the ground motion recorded at the bottom most layer for deep and shallow profiles. Using linear mixed effect models on residuals calculated from recorded and predicted surface spectra, fixed bias and σ are calculated. Layer having $V_s \geq 1500$ (± 150) m/s is suitable for capturing the surface amplification spectra for both deep and shallow deposits.

1. Introduction

Site amplification due to the presence of deep and shallow local soil profiles plays a vital role in estimating the surface hazard values at any given site. The depth of local soil deposits can modify the seismic waves, which influences the ground motion and ultimately leads to structural damage. 1987, Mexico earthquake; 1989, the Loma Prieta earthquake; 1995 Kobe earthquake; 2001 Bhuj earthquake; 2010 Canterbury earthquake and 2015 Nepal earthquake are the classic examples that emphasise the influence of site amplification due to local site effect. Depth at which the input ground motion is given to estimate site-specific response parameters of in-situ soil deposits with limited seismic bedrock information is the most significant in seismic design. Most of the researchers (Bakir *et al.* 2002, Hough *et al.* 2011, Bradley and Cubrinovski 2011) have concluded that softer materials near the free surface govern the damage pattern at short distances. Various projects (NGA WEST GMPEs project) incorporated site effects using the time average shear wave velocity at 30 m depth. However, in all important projects, a detailed site response analysis of the site needs to be performed. Hence, modelling the non-linear behaviour of soil is a vital component. However, a limited number of observations are available for studying the influence of the layer of input motion on surface amplification spectra.

In general, a one-dimension (1D) site response analysis is used, where the wave propagation equation is resolved for a site condition and ground motion. Software such as STRATA, EERA, Shake91, and DEEPSOIL are generally used for site response analysis. In most of the cases, researchers (Govindaraju and Bhattacharya 2012, Kumar *et al.* 2012, Mahajan *et al.* 2007, Anbazhagan and Sitharam 2008, Fattah *et al.* 2018, Omar *et al.* 2013, Abdullah *et al.* 2018; Al–Damluji *et al.* 2002) have either used 760 m/s or 30 m depth or top of bottommost investigation layer for inputting the ground motion irrespective soil deposit thickness. It can be noted that most of GMPEs are developed for seismic bedrock level with shear wave velocity 1500 m/s and above. Anbazhagan *et al.* (2013) noted the influence of depth of inputting ground motion for shallow profiles considering synthetic profiles without actually known amplification. The downhole array is one of the effective comparison tools in evaluating the assumptions and capabilities of site response analysis programs. Numerous studies have been carried out using a vertical downhole array, e.g. to identify the effectiveness of computational models, the dynamic behaviour of soil. Similarly, Bradley (2011) presented the framework for validation and uncertainty associated with various computational models using the observations from the

---

Correspondence to P Anbazhagan ✉ anbazhagan@iisc.ac.in ⊕ Department of Civil Engineering, Indian Institute of Science, Bangalore, 560 012 India.
080-22932467
⊕ Supplemental data for this article can be accessed here.

seismometer array. Thompson *et al.* (2012) performed considerable site response analysis on KiK-Net (Kiban-Kyoshin Network) array using low amplitude ground motion and identified 16 profiles for which assumption of 1D SH (horizontally polarises shear wave) are valid. Kaklamanos *et al.* (2013) used KiK-Net profiles and determined the critical parameters affecting bias and variability in site response analysis. Further, Kaklamanos *et al.* (2015) used KiK-Net profiles in comparing the nonlinear and equivalent linear total stress site response and found out the dependency on assumed model reduction and damping curves. Additionally, Anbazhagan *et al.* (2017) and Bajaj and Anbazhagan (2020) used KiK-Net sites in the identification of suitable shear modulus reduction and damping curves for rock, gravel and clay sites for reliable estimation response parameters. Most of these studies input ground motion was given at the recorded layer of seismic bedrock. However, measuring dynamic properties up to seismic bedrock is expensive or not possible in deep soil deposits for seismic microzonation. Hence, in this study, the downhole array of KiK-Net sites has been used for determining the input layer depth or velocity for capturing the proper amplification spectra at the surface.

The paper aims to study the effect of inputting the ground motion at different depth and velocity layers on the surface amplification spectra. For this purpose, recorded ground motions at both bedrock and surface from KiK-Net downhole array have been carefully selected for the study. The recorded ground motion at bedrock is given as input at different layers starting from the recorded layer while keeping the other parameters constant. The response at the surface has been predicted using 1D nonlinear site response analysis. Predicted response at the surface is compared with the recorded surface amplification spectra by parametrically varying the depth and velocity for inputting recorded ground motions. Linear mixed-effect model is used on residuals calculated from predicted and surface recorded amplification spectra. Bias and standard deviation for all the input curves are determined and compared, and the best representative input motion depth and velocity have been suggested. The suggested inputting ground motion depth and velocity can be used for the sites where bedrock depth is not available for both deep and shallow profiles.

2. Ground motions and sites selection for analysis

The profiles used in this study are collected from the Kiban-Kyoshin network (KiK-Net, K-Net, http://www.kyoshin.bosai.go.jp/). The KiK-Net and K-Net were authorised in 1996 and are operated by the National Research Institute for Earth Science and Disaster Prevention (NIED) after the 1995 Kobe earthquake. Among more than 1000 observation stations, only 700 have downhole and surface high-quality seismographs. Surface-source downhole logging is conducted to acquire the shear wave velocities (V_s) at each depth. Additionally, a period of its origin and major type of soil is also available at each depth for the respective site. For each of the selected profiles, pairs of acceleration time histories for both the horizontal components at the site are obtained from KiK-Net database. The recorded ground motions with surface recording peak ground acceleration (PGA) greater than 0.05 g is used in the analysis. The methodology proposed by Dawood *et al.* (2016) is used in processing the collected ground motions and a high-pass fourth-order acausal Butterworth filter was employed as per Boore and Bommer (2005) using the Boore Fortran Programs (TSSP). The corner frequencies are picked through the procedure developed by Dawood *et al.* (2016), acquired from the corresponding NEES flat file for all the KiK-Net sites.

Thompson *et al.* (2012) studied the KiK-Net downhole array and used 100 sites with 4862 ground motions recorded from 1573 earthquakes with a surface acceleration of less than 0.1 g. From 100 selected sites, 16 were identified as a good fit for one-dimensional horizontally polarised shear wave propagation (1D SH) and had low intraevent variability and a good fit for 1D SH assumptions (LG). 53 were identified as a poor fit for 1D SH assumption (LP), stating that these profiles required non-linear modelling. Out of 100 profiles used by Thompson et al. (2012), for only 16 profiles have the depth of bedrock is more than 70 m which were defined by Kaklamanos *et al.* (2013). Out of 16, only six profiles were considered. Out of six profiles, four are classified as LP profiles (Thompson *et al.* 2012). Most of the profiles considered by Thompson *et al.* (2012) were either having sand or gravel lying over the rock as the predominant soil type. Hence, in addition to these six profiles, eight other profiles, including clay and silt as their predominant soil type are selected. These profiles have low intraevent variability. Hence, non-linear site response analysis is considered. Similar to Thompson *et al.* (2012), KiK-net stations having ten records where the minimum signal to noise ratio of more than five between 0.5 to 20 Hz bandpass was only used for analyses. Selection criteria result in 309 ground motions from 14 deep soil profiles. The summary of the profiles used in the study is given in Table 1. Additionally, shallow profiles are also used for selecting the effective depth for site response analysis. Four rock sites (i.e.

IWTH05, FKSH18, IWTH08, IWTH27); one gravel site (i.e. FKSH11); and two sand sites (FKSH08, TCGH15) are considered similar to Anbazhagan *et al.* (2017). Additionally, three clay predominant sites (IWTH02, SITH11, KSRH10) and two gravel predominant sites (FKSH11, IBRH18) are also considered similar to Yang *et al.* (2017). Details about the selection of sites are given in respective studies. Selection criteria result in 285 ground motions from 13 shallow soil profiles. A summary of all these shallow sites is presented in Table 2.

The downhole logging and peak picking are used for obtaining the travel times and further to get the shear wave velocity (V_s) profiles for KiK-net sites. Thompson *et al.* (2012) observed the difference in V_s structure while comparing the V_s profiles estimated through spectral analysis of surface waves and KiK-Net database. Even though uncertainty in downhole logging is less, but in this study, we assume that soil heterogeneity and inaccurate V_s structure is the major source of misfit of the 1D SH wave propagation assumption.

This issue is addressed using Monte Carlo simulations for varying V_s structure and carrying detailed linear site response at LP sites using low amplitude ground motions (PGA~0.05 g). For all the simulated profiles, response spectra are obtained and compared with the geometric mean of the recorded response spectra at the top of the deposit. Pearson's correlation coefficient (R^2) is used in ranking the profiles. V_s profile which is comparable to the seed profile retrieved from KiK-Net database and having high R^2 is further used in the analysis. Obtaining the variation of small strain damping with depth is a major factor in linear site response study; however, various authors (e.g. Park and Hashash 2005) have proposed different methodologies to obtain it. Small strain damping values are varied in each layer of the simulated profiles obtained from Monte Carlo simulations. Average small stain damping value for respective V_s profile is provided as a seed value of the small strain damping (Kaklamanos *et al.* 2015). The whole procedure is explained with an example in Appendix A.

Table 1. Description of deep soil profile used in this study.

S. No.	Site	Available Soil Type till Z_{BR}	Predominant Soil Type	Class as per Thompson *et al.* (2012)	Z_r	Z_{BR}	n	V_{s30}	NEHRP site classification	Max PGA (g) at Z_r	Range of PGA (g) at the surface
1	AICH05	Clay + Sand	Clay	-	404.6	364	10	301	D	0.04	0.019–0.12
2	AOMH17	Sand + Clay	Sand	-	117	74	23	378	C	0.08	0.04–0.29
3	EHMH04	Sand + Clay + Gravel	Gravel	LP	200	94	10	254	C	0.14	0.01–0.32
4	IBRH17	Sand + Silt + Gravel	Sand + Silt	LG	510	134	50	301	D	0.17	0.02–0.42
5	KMMH03	Rock	Rock	-	203	-	12	280	D	0.15	0.02–0.78
6	KMMH14	Gravel + Rock	Gravel	-	113	83	50	248	D	0.15	0.04–0.45
7	KSRH05	Gravel + Rock	Rock	LP	330	-	20	389	C	0.01	0.02–0.29
8	MIEH10	Silt + Gravel	Silt	-	197	70	10	422	C	0.33	0.02–0.85
9	SZOH42	Clay + Sand + Rock	Sand	LP	203	128	15	153	E	0.11	0.01–0.44
10	SZOH43	Silt + Sand	Sand	-	242	156	10	323	D	0.09	0.03–0.24
11	TCGH10	Gravel	Gravel	LP	132	100	50	371	C	0.20	0.02–0.60
12	TKCH08	Gravel	Gravel	LG	353	78	25	353	D	0.12	0.01–0.50
13	YMTH04	Gravel + Rock	Rock	-	103	-	14	248	D	0.03	0.02–0.22
14	YMTH06	Clay + Gravel	Clay	-	148	128	10	261	D	0.05	0.01–0.20

Z_r: – Depth of downhole sensor (m); Z_{BR}:- Depth of Bed Rock (m); n: – number of ground-motion; V_{s30}: – time average shear wave velocity at top 30 m depth

Table 2. Description of shallow soil profile used in this study.

S. No.	Site	Available Soil Type till Z_{BR}	Predominant Soil Type	Class as perThompson *et al.* (2012)	Z_r	Z_{BR}	n	V_{s30}	NEHRP site classification	Max PGA (g) at Z_r	Range of PGA (g) at the surface
1	IWTH05	Rock	Rock	LP	103.3	-	20	429	C	0.17	0.09–0.81
2	FKSH18	Rock	Rock	LP	103	-	20	307	D	0.04	0.05–0.35
3	IWTH08	Rock	Rock	LG	103	-	20	305	D	0.04	0.03–0.37
4	IWTH27	Rock	Rock	LG	103	-	30	670	C	0.14	0.05–0.76
5	FKSH11	Gravel + Rock	Gravel	LG	118.2	35	20	240	D	0.12	0.02–0.27
6	IBRH18	Gravel + Rock	Gravel	LP	504	32	30	559	C	0.15	0.03–0.60
7	NIGH12	Gravel + Rock	Gravel	LP	110	52	30	553	C	0.12	0.03–0.30
8	TCGH15	Sand + Rock	Sand	LP	300	21	30	423	C	0.07	0.04–0.34
9	FKSH08	Sand + Rock	Sand	LP	108	50	10	563	C	0.04	0.04–0.13
10	SITH11	Clay + Rock	Clay	-	104	14	10	372	C	0.02	0.03–0.20
11	IWTH02	Clay + Rock	Clay	LG	102	15	20	390	C	0.04	0.04–1.09
12	KSRH10	Clay + Rock	Clay	LG	213	35	30	213	D	0.12	0.03–0.58

Z_r: – Depth of downhole sensor (m); Z_{BR}:- Depth of Bed Rock (m); n: – number of ground-motion; V_{s30}: – time average shear wave velocity at top 30 m depth

Another important factor required for site response is the in-situ density of the subsurface layers of KiK-net profiles database. Since in-situ density was not available in the KiK-net profile and it has been estimated here. Gardner *et al.* (1974) developed a widely used correlation between shear wave velocity and in-situ density but is valid for the sites with V_s more than 1524 m/s. Anbazhagan *et al.* (2016) developed a correlation between V_s and in-situ density and compared with the correlations developed by Gardner *et al.* (1974) and Inazaki (2006) and concluded a good agreement in all these relations. In this study, the in-situ density of each layer is estimated using the relationship developed by Anbazhagan *et al.* (2016) with $\pm 1\sigma$. Numerous studies (Grelle and Guadagno 2009) have found that P-wave velocity (V_P) of 1000–2000 m/s are characteristic of saturated soil. Hence, similar to Kaklamanos *et al.* (2015), the ground water table is assumed where V_P first surpasses 1500 m/s. The coefficient of lateral earth pressure at rest (K_o) is computed using the theoretical relationship between K_o and Poisson's ratio (v) i.e. $K_o = v/(1-v)$, where $v = \left(V_p^2 - 2V_S^2\right)/\left(2V_p^2 - 2V_S^2\right)$. Other model parameters used are described further.

3. Methodology

Site response analysis has been carried out using DEEPSOIL (Hashash *et al.* 2017). Both equivalent linear total stress and non-linear site response analysis have been performed for the identification of shear wave velocity profiles. For performing linear site response and Monte Carlo trials for calibrating LP sites, STRATA has been used. Initially, all profiles are calibrated by giving input at the recorded level, V_s profile from Monte Carlo simulation and fixing density and shear modulus and damping curves. Considering the best match between predicted and recorded response spectrum, all the input parameters were frozen and further used for depth analysis. For the given set of input parameters and ground motion, the input level was changed, and response is predicted at the surface. The predicted response is further compared with the recorded response at the surface.

For determining the goodness-of-fit for different input motion depths, the observed response spectra at the surface, $SA_{obs}(T)$, is compared with the predicted response spectra at the surface, $SA_{pred}(T)$ from site response study using DEEPSOIL. The residual between the observed and obtained SA (5% damping) is natural logarithm space as

$$SA_{resid}(T) = \ln[SA_{obs}(T)] - \ln\left[SA_{pred}(T)\right] \qquad (1)$$

Where the geometric mean is used to combine the two orthogonal horizontal components of recorded ground motion. Negative and positive residuals respectively indicate as over predictions and underpredictions. For properly acquiring the statistical significance of different input motion depths, the dependency between multiple recordings at a single site needs to be evaluated. Mixed-effect regression (Pinheiro and Bates 2000) is a statistical procedure that helps in evaluating the repeatable bias and variance when the data are grouped into one or more classification factors. In this study, the data is grouped by different input depths. The mixed-effect model incorporates both fixed effects and random effects i.e. the parameter associated with an entire population and units drawn at random from the population, respectively. Using mixed-effect regression models, parameter at the specific spectral period, T can be modelled as

$$SA_{resid}(T)_{i,j} = \alpha + \eta_{si} + \in_{i,j} \qquad (2)$$

here, α is the population mean of $SA_{resid}(T)$, i.e. fixed effect, which represents the average bias in shear modulus and damping curves along with ground motions; η_{si} and $\in_{i,j}$ are the inter-site and intra-site residuals respectively. η_{si} and $\in_{i,j}$ respectively represent the deviation from the population mean of the mean residual for the i th site and deviation of ground-motion observation j at site i from the mean residual at site i. Both inter, and intra-site residuals are normally distributed with zero mean random variables and τ_s and σ_o are respective standard deviation. The pictorial representation and detailed explanation of the methodology used are given in Bajaj and Anbazhagan (2018). This mixed-effect model is used for examining the precision and bias in input level depths used in site response analysis.

4. Shear modulus reduction and damping curves used

Various researchers have developed numerous shear modulus reduction and damping curves with different shear strain values and for different materials. For all the available shear modulus reduction (G/G_{max}) and damping ratio curves for the soil in the literature, a set of curves are widely used by researchers in site response analysis. G/G_{max} and damping ratio curves presented by Seed and Idriss (1970), Seed *et al.* (1986), Vucetic and Dobry (1991), EPRI (1993), Ishibashi and Zhang (1993),

Rollins *et al.* (1998), Darendeli (2001), Menq (2003), and Zhang *et al.* (2005) are widely used for representing the dynamic behaviour of the soil column.

Using the KiK-net downhole array, Anbazhagan *et al.* (2017) have suggested the G/G_{max} and damping ratio of sand, gravel and rock predominate profiles. Kaklamanos *et al.* (2015) used G/G_{max} and damping ratio proposed by Darendeli (2001) and Zhang *et al.* (2005) for carrying out site response analysis for KiK-Net sites. Whereas, Anbazhagan *et al.* (2017) proposed EPRI (1993), Seed and Idriss (1970) upper limit and Rollins *et al.* (1998) (-SD) G/G_{max} and damping ratio for rock, sand and gravel predominant soil. However, most of the sites used by Anbazhagan *et al.* (2017) are shallow and rock dominated. Hence, Bajaj and Anbazhagan (2020) used both shallow and deep profiles from KiK-net downhole array and suggested the representative curve for clay, sand, gravel, and rock predominate profiles. Based on the analysis on residuals, Bajaj and Anbazhagan (2020) suggested Electric Power Research Institute (EPRI) (1993), Menq (2003), Zhang *et al.* (2005) and Darendeli (2001) G/G_{max} and damping ratio for rock, gravel, sand and clay predominate profiles respectively.

Based on the predicted and recorded surface spectra, in this study, Electric Power Research Institute (EPRI) (1993) G/G_{max} and damping ratio for rock deposits are used. For gravel predominant soil deposits Menq (2003) G/G_{max} and the damping ratio are used. Menq (2003) have been used by varying $0.2 \leq D_{50} < 5$ and $1.1 \leq C_u < 10$ based on the density of the deposition, D_{50} and C_u represent the median grain size and coefficient of uniformity respectively (Bajaj and Anbazhagan 2020). PI is considered 0 for sand, 15 to 20 in case of silt and 30 to 60 in clay. Further, for clay deposits, Darendeli (2001) is used with PI (Plasticity Index) range 40 to 60 in case of deep clay deposits and 30 to 50 in case of shallow clay deposits (Kaklamanos *et al.* 2015, Bajaj and Anbazhagan 2020). In the case of silty deposits, Darendeli (2001) G/G_{max} and the damping ratio is used with a PI range from 20 to 30 (Bajaj and Anbazhagan 2020). For Zhang *et al.* (2005), geological profiles are taken from KiK-Net website. These curves are further kept constant and used in determining the depth of the input motion.

5. Brief overview of bedrock depth for input ground motion

Defining the input level for ground motion plays an essential role in the precise quantification of site amplification. Most researchers have used different depths for applying the input ground motion for the site response study, but there is no guideline or study about the same. However, the impact of deep soil deposits on surface amplitude spectra has been observed by various authors (e.g. Hashash and Park 2001, Akin *et al.* 2016). Hence inputting ground motion at any depth may change the amplification factor and surface amplification spectra at different frequencies in the same site.

Akin *et al.* (2016) used the boundary between NEHRP site classes B and C, i.e. 760 m/s, as bedrock shear wave velocity also as an input level for site response analysis of Erbaa. Ansal and Tonuk (2007) stated that V_s profiles should be defined down to the depth of engineering bedrock with estimated V_s of 700–750 m/s. Many studies (Park *et al.* 2004, Park and Hashash 2005, Cramer 2006) have questioned NEHRP site coefficients' validity for the regions having thick deposits such as Mississippi embayment. Hashash *et al.* (2008) developed the soil-column depth-dependent seismic site coefficient by using bedrock at 30 m, 100 m, 200 m, 300 m, 500 m and 1000 m. For the soil profiles thicker than 30 m, the derived site coefficients are lower at short periods and higher at long periods as compared to NEHRP site coefficients (Hashash *et al.* 2008). Malekmohammadi and Pezeshk (2015) used four bedrock depths i.e. 70 m, 140 m, 400 m and 750 m for site response analysis of Mississippi embayment. Kwok *et al.* (2008) fixed the bedrock below 23 m, having V_s more than 760 m/s for ground response analysis of Turkey Flat, shallow stiff-soil sites. Silva (2008) carried out the site response study for a range of soil profiles parameterised by V_{s30} and the depth to $V_s = 1000$ m/s.

Chapman and Talwani (2002) defined rock model for South California as (1) realistic geologic condition and consisted of very thick outcrop soft-rock (V_s=700 m/s) layer over hard rock and (2) hard-rock outcrop condition, consisting of 250 m of weathered hard rock (V_s=2500 m/s) underlined by a half-space of un-weathered hard rock (V_s=3500 m/s). Anbazhagan *et al.* (2013) have observed no significant difference in response spectra at the surface when ground motion is inputted at bedrock having V_s between 1385 to 1868 m/s, for shallow sites. However, the significant difference is shown when the input ground motion acceleration is applied at 30 m depth and bedrock level (Anbazhagan *et al.* 2013). On studying the uncertainties on site response, Barani *et al.* (2013) concluded that soil thickness plays a vital role in those places where bedrock depth is unknown or largely uncertain. In the absence of the hard rock depth, most of the studies applied input ground motion either layer with $V_s \geq 700$ m/s or 30 m depth or top of the bottom most layer of investigation. Change of input level/layer and its effect on the response spectrum is discussed in the section for deep soil sites. KiK-Net sites recorded spectra are available at both surface and bedrock are

ideal data to study the effect of the input layer and establish input level after analysis of several profiles. Hence in this study, the input is given at different depths and residual for recorded and predicted response spectra at the surface is calculated for KiK Net data. Based on the residual input layer shear wave velocity/depth has been suggested.

6. Effect of input layer depth and velocity on surface amplification

Till date, very few studies have presented the impact of input layer depth and velocity on-site amplification. However, for the sites with unknown bedrock depth, inputting the motion at a random layer may result in a biased estimation of surface amplification. Hence, a typical example of deep site SZOH43 and shallow site IWTH27 is taken to see the impact of input layer depth and velocity on surface amplification. Initially, both the sites have been calibrated for soil condition (i.e. type of soil, G/G_{max} and damping ratio curves and pore water pressure) by matching the predicted and recorded surface spectrum. For calibrating, the input motion is given at recorded bedrock depth, i.e. D=242 m, V_s=1080 m/s and D=103 m, V_s=2790 m/s in case of SZOH43 and IWTH27 respectively.

Depth of SZOH43 site is 242 m and V_s of the bottom most layer is 1080 m/s and the thickness of this layer is 62 m. Hence this layer is divided into two-part and input motion is given at these two different depths (i.e. 242 and 186 m) and surface response spectra are derived. Similarly, the procedure has been adopted for the other layers until V_s equals to 750 m/s at a depth of 37 m. Typical variation of response spectra and average residuals at different spectral periods for SZOH43

profile is given as Figure 1(a,b) respectively. A similar analysis has been done for shallow sites. IWTH27 is divided into four parts, i.e. 2790, 2790, 1950 and 1100 m/s at depth 103, 62, 46 and 16 m respectively, based on the thickness of each layer. A typical example for IWTH27 is given as Figure 2. With the decrease in depth of input motion, in addition to an increase in amplification, a significant amount of change in the time period is also observed especially in case of deep deposits. With the decrease in velocity from 1080 m/s to 750 m/s (SZOH43), dual peaks in response spectra are observed. Due to a change in velocity and depth of the input layer, a significant amount of change in the frequency of the soil column is observed. As the input level of motion changes, a shift in peak is also observed (see Figure 1). In general, the depth of input motion is considered to be either 30 m or 760 m/s velocity layer. However, with this analysis, it is also observed that inputting at 37 m/750 m/s may result in biased response spectra at the surface especially in the case of deep sites. Hence, it is necessary to arrive at a depth or velocity of the input layer for the site response study with unknown bedrock depth.

7. Analysis of depth

In this study, using the KiK-Net profiles, the recorded ground motions are inputted at different depths, and the surface spectra are obtained. The input motion depth dependency is analysed to get a clear picture of the depth effect on surface response spectra in response analysis. The bias is calculated using input depth as a random variable and data are grouped according to residual calculated for different time periods. Using equation 2, (a) fixed effect, α; (b) intra-site/curve
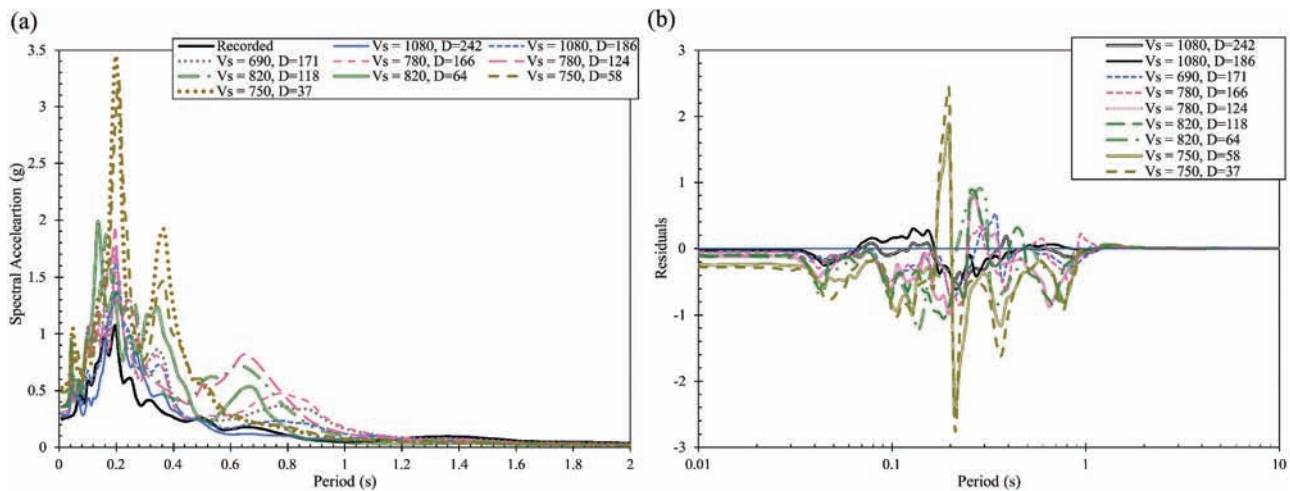
Figure 1. Variation of (a) response spectra and (b) residual for inputting motion at different depths for SZOH43. Residuals plotted are the average residuals considering 10 ground motions recorded at SZOH43 sites. Velocity (Vs) is in m/s and depth (D) is in m.
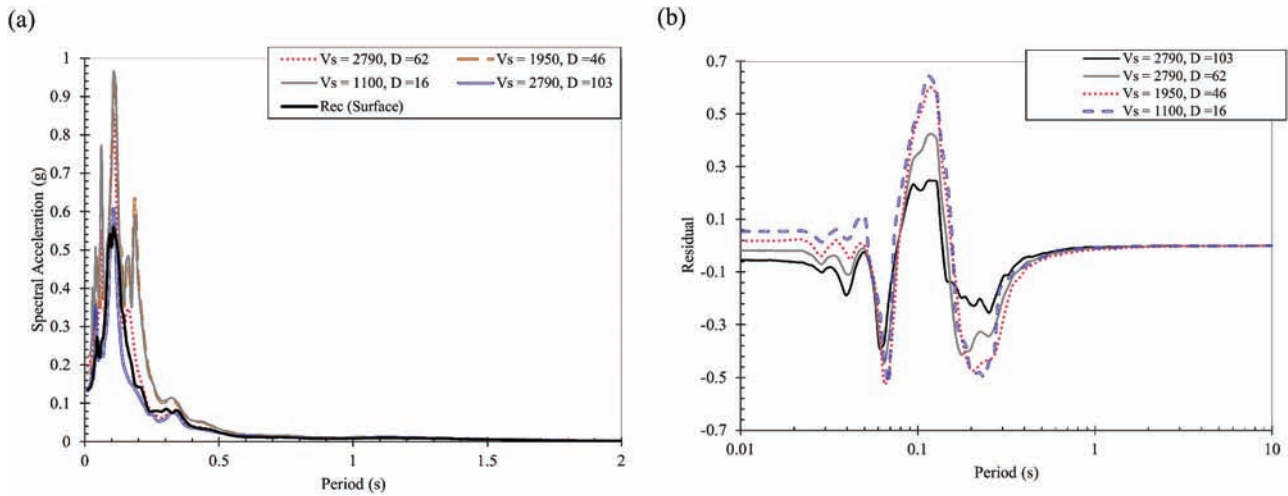
Figure 2. Variation of (a) response spectra and (b) residual for inputting motion at different depths for IWTH27. Residuals plotted are the average residuals considering 30 ground motions recorded at IWTH27 sites. Velocity (Vs) is in m/s and depth (D) is in m.

standard deviation, σ_o; (c) inter-site/curve, τ_s; and (d) total standard deviation, σ_Y have calculated using the mixed-effect regression model.

Tables 3 and 4 give the overview of the different input ground motion layers at different depths used for analysis. For example, AOMH17, the depth of the site 117 m and V_s of the bottom most layer is 1450 m/s and the thickness of this layer is 42 m. Hence for this layer is divided into three parts and input motion is given at these three depths (i.e. 117, 107 and 83.75 m) and surface response spectra are derived. Similarly, for the second layer of thickness 45 m and V_s 770 m/s, input motion is given at three different depths and surface spectra are predicted. Typical variation of response spectra and average residuals at different spectral periods for AOMH17 profile is given as Figure 3(a,b) respectively. A similar procedure has been adopted for all the deep and shallow profiles used in this study and residuals has been calculated by inputting ground motion at different layers (see Tables 3, 4).

Figure 4 typically shows the variation of actual and intra residuals considering different depths as a random variable for AICH05 site. Average residual has been calculated by inputting different rock recorded ground motions at different depths corresponding to different velocities. Using the mixed effect models, bias and standard deviation have been calculated for giving input motion at different depths (mentioned in Tables 3, 4). The calculated bias and standard deviation for different deep sites are given in Table 3. Bias value (fixed effect) at 1450 m/s (117 m), 1450 m/s (107 m), 1450 m/s (83.75 m), 770 m/s (75 m), 770 m/s (55.5 m) and 770 m/s (36 m) respectively is −0.00858, −0.0021, 0.00112, 0.00498, −0.01215 and 0.02761. The fixed

effect, $a = -0.00858$, means the average value of spectral acceleration residual across all the time periods and ground motion records is −0.00858, or the average of spectra acceleration observed and predicted is equal to $\exp(-0.00858) = 0.98$. Based on the observed bias value at different depths and velocities for AICH05, it can be concluded that as the depth of input ground motion is decreasing, in most of the cases, it starts underpredicting the spectral acceleration value. The variation of intra-site residual with spectral periods is almost constant before 0.04 and after 1 s, which means changing the input level depth significantly affects the spectra period between 0.1 to 0.6 sec (see Figure 4c). A detailed discussion about this is given later. Similarly, the standard deviation is also calculated for all the input level depths, which increases with the decrease in input motion depth (see Table 3 for AICH05). Similar to AICH05, for all other sites (see Table 1) residuals have been studied by dividing them into bias, intra-site and inter-site residuals and variation has been studied for different depths. The variation of actual and intra-site residuals for all the deep sites is given as Appendix Figure A1 (1) to A1 (13) (submitted as an electronic supplement). The calculated bias and standard deviation for different deep sites for different input levels are given in Table 3.

Figure 5 typically shows the variation of actual and intra residuals considering different depths as the random variable for IWTH27 site, which is a shallow site. Similarly, using the mixed effect models, bias and standard deviation have been calculated for giving input motion at different depths (mentioned in Tables 3, 4). The calculated bias and standard deviation for different shallow sites are given in Table 4. Bias value (fixed

Table 3. Bias and Standard deviation calculated by inputting ground motion at different depths and velocity layers for deep sites.

S. No.	Site	Depth	Velocity (m/s)	Standard deviation	bias
1	AICH05	404.6	730	0.0240	−0.0023
		312.3	730	0.0353	0.0047
		224.7	730	0.0502	0.0095
2	AOMH17	117	1450	0.0239	−0.0086
		107	1450	0.0330	−0.0021
		83.75	1450	0.0377	0.0011
		75	770	0.0391	0.0050
		55.5	770	0.0501	−0.0121
		36	770	0.0574	0.0276
3	EHMH04	200	755	0.1113	0.0072
		159	750	0.1312	−0.0090
		115	750	0.1668	0.0289
		71	750	0.2052	0.1130
4	IBRH17	510	2300	0.0136	−0.0070
		476	2300	0.0188	−0.0035
		456	820	0.0246	−0.0064
		425	820	0.0404	−0.0053
		395	820	0.0541	−0.0048
5	KMMH03	200	2000	0.0633	0.0276
		167	2000	0.0945	−0.0073
		131	2000	0.0999	0.0052
		128	1300	0.1108	−0.0281
		116	1300	0.1219	0.0286
		92	1300	0.1443	0.0102
6	KMMH14	113	1540	0.0382	0.0158
		100	1540	0.0684	0.0245
7	KSRH05	330	800	0.1541	−0.0453
		308	800	0.2192	−0.0216
		284	800	0.2215	−0.0244
8	MIEH10	200	990	0.0349	0.0027
		173	990	0.0384	−0.0010
		156	990	0.0395	−0.0076
		148	850	0.0416	−0.0265
		110	850	0.0551	−0.0228
		79	850	0.0699	−0.0200
9	SZOH42	203	970	0.0667	−0.0119
		172	970	0.0870	0.0004
		148	970	0.0902	0.0062
10	SZOH43	242	1080	0.1127	−0.0270
		186	1080	0.1323	−0.0426
		171	690	0.1536	−0.0926
		166	780	0.1487	−0.0917
		124	780	0.2116	−0.1589
		118	820	0.2111	−0.1544
		64	820	0.2336	−0.1295
		58	750	0.3975	−0.2504
		37	750	0.4127	−0.2737
11	TCGH10	132	820	0.1311	0.0373
		100	820	0.1643	−0.0108
		68	820	0.2957	−0.0936
12	TKCH08	103	2800	0.0990	−0.0045
		85	2800	0.1089	−0.0005
13	YMTH04	103	1090	0.0578	−0.0198
		92	1090	0.0821	−0.0128
14	YMTH06	148	1090	0.0655	0.0138
		128	730	0.0771	0.0454
		92	730	0.0919	0.0593

Table 4. Bias and Standard deviation calculated by inputting ground motion at different depths and velocity layer for shallow sites.

S. No.	Site	Depth	Velocity (m/s)	Standard deviation	bias
1	FKSH18	103	1909	0.0288	0.0025
		49	1909	0.0400	0.0192
2	IWTH05	103	2600	0.0540	0.0789
		48	2600	0.0822	0.0242
		37	1500	0.0927	−0.0784
		26	850	0.0860	0.1301
3	IWTH08	103	2120	0.0389	0.0242
		50	2120	0.0636	0.0121
		34	900	0.0612	−0.0038
4	IWTH27	103	2790	0.1053	−0.0808
		62	2790	0.1558	−0.0675
		46	1950	0.1981	−0.0543
		16	1100	0.2054	0.0284
5	FKSH11	118	700	0.0390	0.0263
		85	700	0.0467	−0.0110
6	IBRH18	507	2200	0.1297	0.0084
		470	2000	0.1329	0.0286
		400	2000	0.1367	0.0757
		390	1900	0.1713	0.0917
		310	1900	0.1780	0.0102
		300	1700	0.1781	−0.0382
		200	1700	0.1792	0.0238
		185	1600	0.2076	0.0896
		70	1600	0.2259	−0.0365
		65	1100	0.2275	−0.2829
		40	1100	0.2775	0.0601
		30	790	0.2769	0.1402
		15	790	0.3325	0.1190
7	NIGH12	113	780	0.0732	0.0112
		85	780	0.0764	0.0065
		60	780	0.0859	0.0151
		50	730	0.0853	0.0413
		30	730	0.0862	0.0119
		14	730	0.1019	0.0271
8	TCGH15	306	1170	0.0115	−0.0006
		249	1170	0.0118	−0.0007
		237	810	0.0121	−0.0010
		189	810	0.0121	0.0039
		181	980	0.0145	0.0023
		110	980	0.0180	0.0051
		34	980	0.0219	0.0039
9	FKSH08	106	1470	0.0289	0.0009
		62	1470	0.0320	−0.0143
		48	900	0.0328	−0.0119
		16	900	0.0339	−0.0083
10	SITH11	104	1801	0.0698	−0.0239
		76	1600	0.1115	0.0108
		44	1350	0.1200	0.0198
		35	1100	0.1332	0.0059
11	IWTH02	105	2300	0.0552	−0.0269
		80	2300	0.0766	−0.0213
		65	2300	0.0932	−0.0059
		58	1900	0.1056	0.0020
		48	1300	0.1102	0.0350
		27	780	0.1240	0.0165
12	KSRH10	258	1700	0.0541	−0.0382
		235	1500	0.0705	−0.0348
		200	1500	0.0955	−0.0088
		190	2000	0.1035	−0.0151
		154	2000	0.1094	−0.0001
		100	2000	0.1123	−0.0034
		80	1400	0.1179	0.0021
		50	1500	0.1216	0.0724

effect) at 2790 m/s (103 m), 2790 m/s (62 m), 1950 m/s (46 m) and 1100 m/s (16 m) respectively is −0.08075, −0.06754, −0.05433 and 0.02839. Based on the observed bias value at different depths and velocities for IWTH27, it can be concluded that as the depth of input ground motion decreases, it starts underpredicting the spectral acceleration value. The variation of intra-site residual with spectral periods is almost constant after 1 s, which means that cis is almost constant after 1 s. Changing the input level depth significantly affects the spectra period below 1 sec (see Figure 5c). A detailed discussion about this is given later. Similarly, the standard deviation is
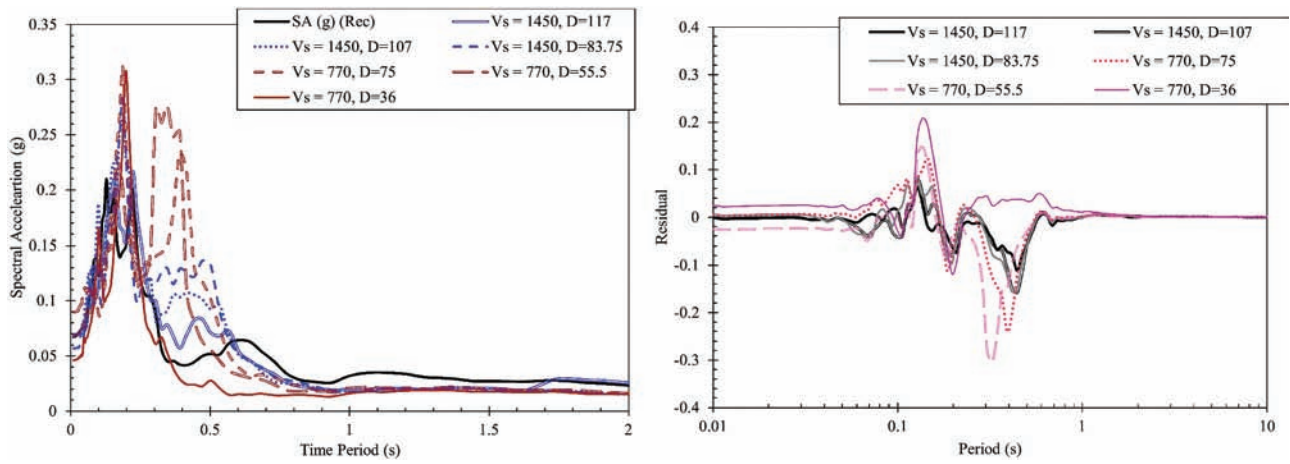
Figure 3. Variation of (a) response spectra and (b) residual for inputting motion at different depths for AOMH17. Residuals plotted are the average residuals considering 10 ground motions recorded at AOMH17 sites. Velocity (Vs) is in m/s and depth (D) is in m.
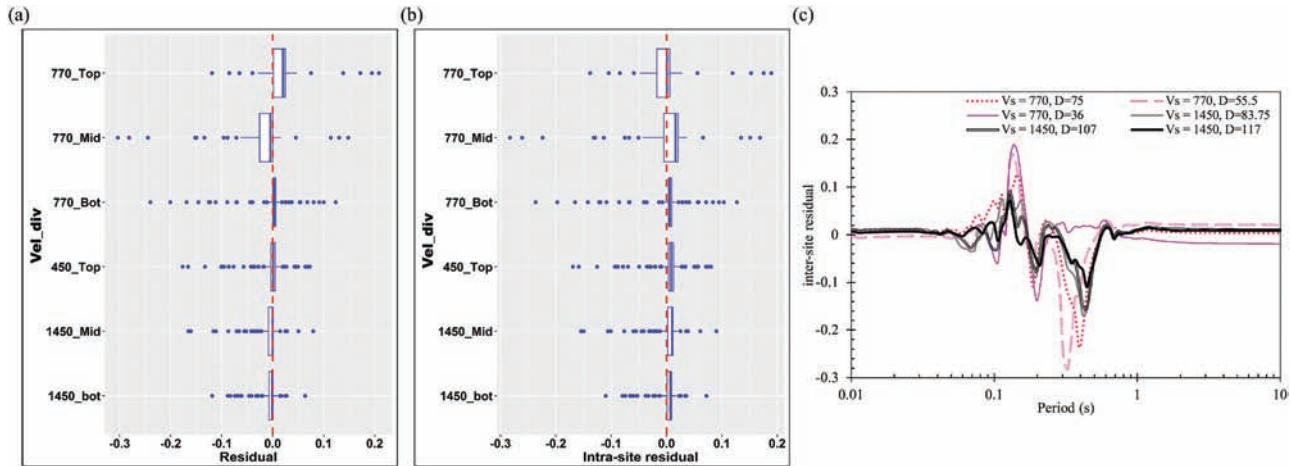
Figure 4. Variation of actual (a) residual, (b) intra-site residual and (c) inter-site residual with spectra period by dividing the shear wave velocity into six parts for AOMH17 site. Velocity (Vs) is in m/s and depth (D) is in m.
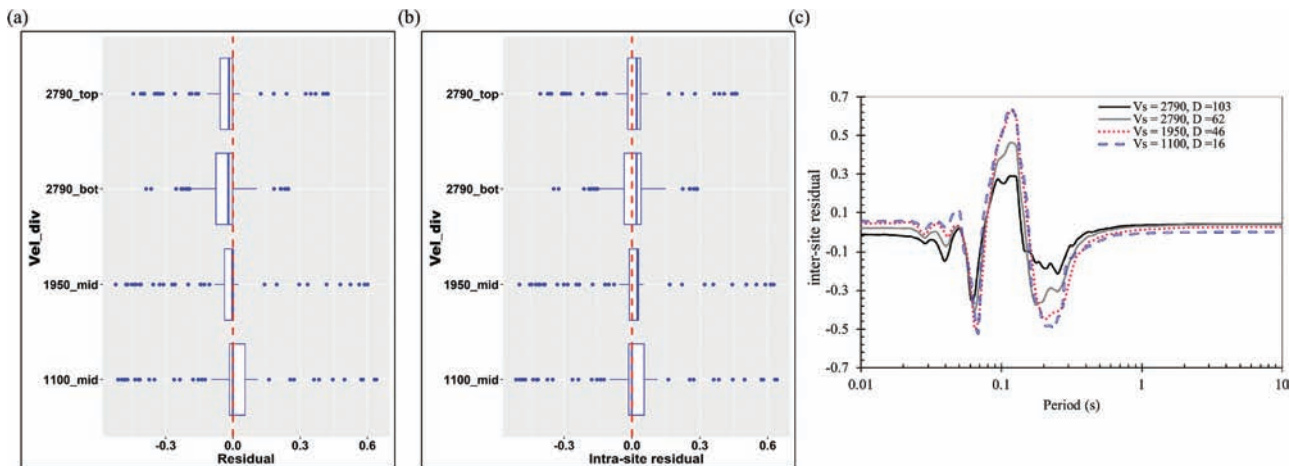
Figure 5. Variation of actual (a) residual, (b) intra-site residual and (c) inter-site residual with spectra period by dividing the shear wave velocity into four parts for IWTH27 site. Velocity (Vs) is in m/s and depth (D) is in m.

also calculated for all the input level depths, which increases with the decrease in input motion depth (see Table 4 for IWTH27). Similar to IWTH27, for all other sites (see Table 1), residuals have been studied by dividing them into bias, intra-site and inter-site residuals and variation has been studied for different depths. The variation of actual and intra-site residuals for all the deep sites is given as Appendix Figure A2 (1) to A2 (11) (submitted as an electronic supplement). The calculated bias and standard deviation for different deep sites for different input levels are given as Table 4. Using mixed effect models on the residuals, bias and standard deviation for different input motion depth has been calculated and given as Tables 3 and 4 respectively for deep and shallow sites.

7.1. Variation of bias and standard deviation for different velocity (depths) for deep sites

Figure 6(a,b) shows the variation of bias and standard deviation for different velocity divisions (see Table 3) for 14 deep sites. Based on the trend of bias and standard deviation, the velocity band (irrespective of depth) is divided into three regions, i.e. RD1, RD2, and RD3 (See Figure 6(a)). The variation of velocity band in these three regions are $700 < RD1 \leq 800$, $800 < RD2 \leq 1000$ and $RD3 > 1000$. It has been seen that for region RD1, the bias and standard deviation are high. For most of the velocity division in RD1, negative bias value has been observed. Overall bias in this region is also negative, which means decreasing velocity overpredicts the spectral acceleration values for most of the time periods. Standard deviation in region R1 is also high with a maximum value of 0.41 at 750 m/s (37 m). The standard deviation for 730 m/s (312.3 m) is less, which

may be due to inputting ground motion at the deeper depth where the nonlinearity of the material has no significant role due to the almost constant stress ratio. In region 2 (after 850 m/s) and region 3, the bias and standard deviation are low. As the velocity increased to 2000 m/s irrespective of depth, the bias value is almost zero. However, a low standard deviation is observed, which may be due to inputting ground motion at lower depth (e.g. 2800 m/s (85 m)). It can be concluded that layer velocity and the depth of inputting ground motion plays a vital role in estimating surface amplification.

Figure 6 shows the variation in bias and standard deviation due to analysing individual profiles. Further, bias and standard deviation have been calculated considering all the depths and velocity division. Using the mixed effect models, bias and standard deviation have been derived considering velocity division (input level at different velocities) as a random variable. It is done to study the effect of depth on inputting ground motion. Figure 7(a–c) shows the variation of bias and standard deviation values with velocity division for region RD1, RD2 and RD3. Further bias and standard deviation have been studied based on different depths. These regions have been divided into three parts, i.e. DD1, DD2, and DD3. The variations of depth band in these three regions are $DD1 \leq 100$, $100 < DD2 \leq 300$ and $DD3 > 300$. Bias and standard deviation for velocity band 730 to 770 and 820 to 920 m/s for DD1 region are significantly high and bias value is almost negative. Further, for 750 to 800 m/s and less than 850 m/s for the DD2 region, bias and standard deviation are relatively high as compared to another velocity band. Irrespective of depth, bias and the standard deviation is almost constant for V_s more than 800 m/s in the DD3 region. A further variation of bias and standard deviation has
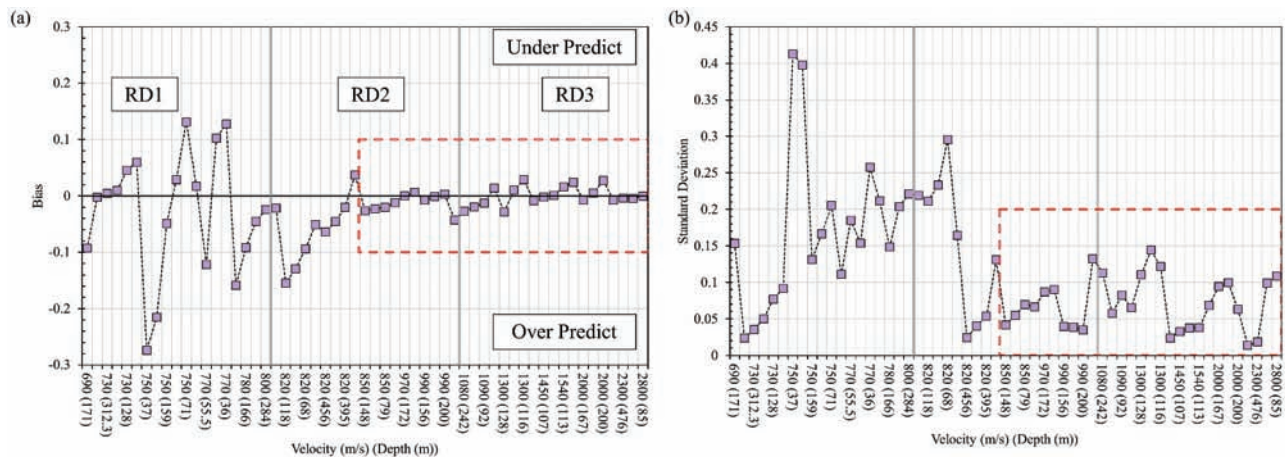
Figure 6. Variation of (a) Bias and (b) Standard deviation with respect to different velocity division considered at different depths for deep sites. Thick vertical lines show the regions (RD1, RD2 and RD3) of variability in these parameters. Dashed box shows the region of less bias and standard deviation.
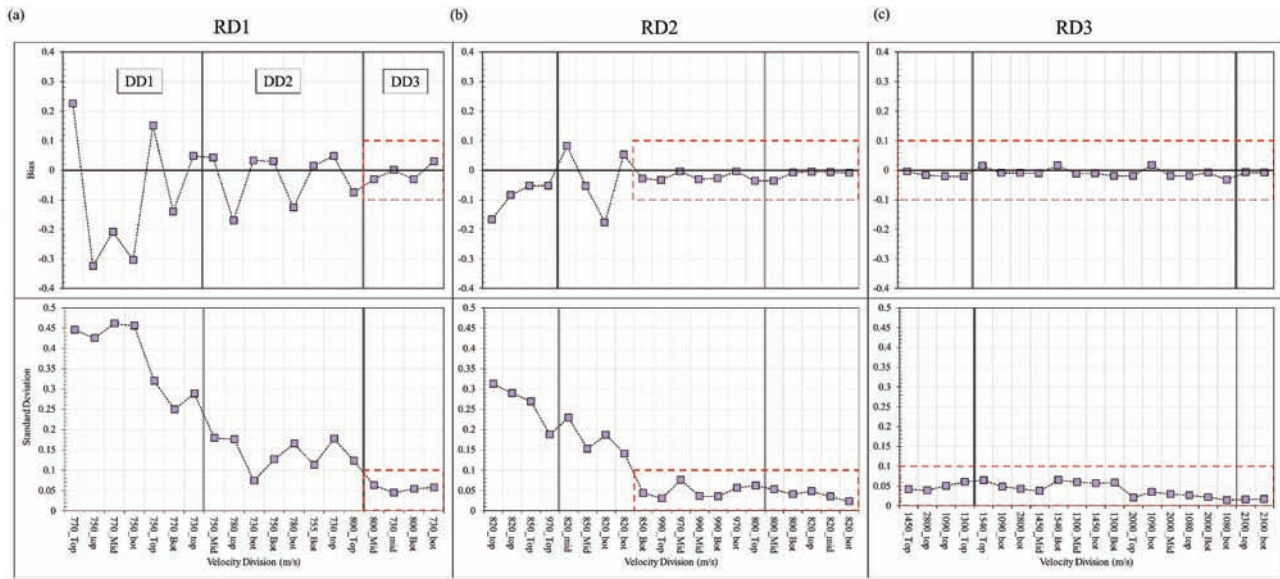
Figure 7. Variation of bias and standard deviation for the region (a) RD1, (b) RD2 and (c) RD3 for different velocity division for deep sites. Thick vertical lines show the regions (DD1, DD2 and DD3) variability of these parameters for different depth division. Dashed box shows the region of less bias and standard deviation.

been studied for different spectral periods. It has been seen that for more than 1 s, the effect of depth of inputting motion has no significant effect. However, for the spectral period between 0.1 to 0.5 s, the variation of bias and the standard deviation is significant and for this period band effect of depth is more on surface amplification (see Figure A3, submitted as an electronic supplement). Based on the overall analysis, it can be suggested for capturing the proper amplification factor at the surface, ground motion can be inputted at the layer having V_s equal to or more than 1500 m/s for deep soil sites irrespective of depths. However, in many deep soil sites for which bedrock level is not known, in that

case, ground motion can be inputted either at a layer having a velocity 1000 m/s and above at a depth of 170 m and above.

7.2. Variation of bias and standard deviation for different velocity (depths) for shallow sites

Figure 8(a,b) shows the variation of bias and standard deviation for different velocity divisions (see Table 4) for 12 shallow sites. Based on the trend of bias and standard deviation, the velocity band (irrespective of depth) is divided into three regions i.e. RS1, RS2, and RS3 (see Figure 8a), similar to deep sites. The variation
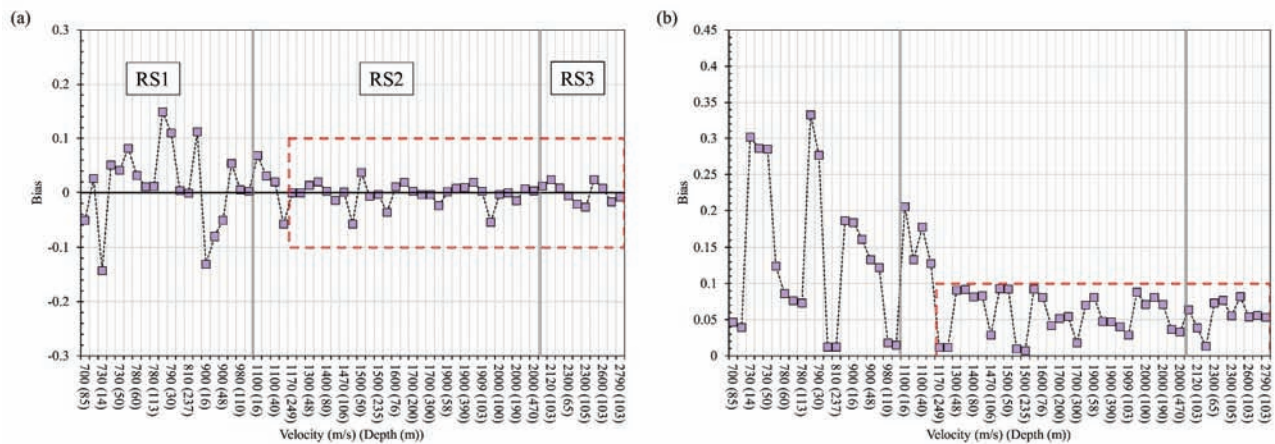
Figure 8. Variation of (a) Bias and (b) Standard deviation with respect to different velocity division considered at different depths for shallow sites. Thick vertical lines show the regions (RS1, RS2 and RS3) of variability in these parameters. Dashed box shows the region of less bias and standard deviation.

of velocity band in these three regions are $700 < RS1 \leq 1000$, $1000 < RS2 \leq 2000$ and $RS3 > 2000$. It has been seen that for region RS1, the bias and standard deviation are high. Unlike RD1, for most of the velocity division in RS1, both negative and positive bias value has been observed. Overall bias in this region is also positive (tends towards zero), which means decreasing velocity is can either overpredict or underpredict the spectral acceleration values for most of the spectral periods, depending upon the depth of input motion. The standard deviation in region RS1 is also high with a maximum value of 0.33 at 790 m/s (15 m). The standard deviation for 780 m/s (113) is less, which may be due to inputting ground motion at a deeper depth where the nonlinearity of the material has no significant role due to the almost constant stress ratio. In region 2 (after 1100 m/s) and region 3, the bias and standard deviation are low. As the velocity increased to 1700 m/s irrespective of depth, the bias value was almost zero. However, the standard deviation is almost constant. Hence, velocity and the depth of inputting ground motion also play a vital role in estimating surface amplification.

Figure 8 shows the variation in bias and standard deviation due to analysing individual profiles. Further, bias and standard deviation have been calculated considering all the depths and velocity division. Using the mixed effect models, bias and standard deviation have been derived considering velocity division (input level at different velocities) as a random variable. It is done to study the effect of depth on inputting ground motion.

Figure 9(a–c) shows the variation of bias and standard deviation values with velocity division for regions RS1, RS2, and RS3. Further bias and standard deviation have been studied based on different depths. These regions have been divided into three parts i.e. DS1, DS2, and DS3. The variation of depth band in these three regions are $DS1 \leq 50$, $50 < D2 \leq 150$ and $D3 > 150$. Bias and standard deviation for velocity band 730 to 790 and for 1100 m/s for DS1 region are significantly high, and bias value is both negative and positive. Further, for 700 to 780 m/s for D2 region, bias and the standard deviation is relatively high as compared to another velocity band. Irrespective of depth, bias, and the standard deviation is almost constant for all velocity divisions in DS3 region. Unlike deep sites, in shallow sites deviation and bias is not tending to zero for velocity less than 2000 m/s and depth less than 150 m. Further, the variation of bias and standard deviation has been studied for the different spectral periods. It has been seen that for more than 1 s, the effect of depth of inputting motion has no significant effect. However, for the spectral period between 0.1 to 0.7 s, a variation of bias and the standard deviation is significant and for this period band effect of depth is more on surface amplification (See Figure A4, submitted as an electronic supplement).

Bias and standard deviation for velocity and depth more than 1500 (−150) m/s and 100 (−15) m, the effect of inputting motion of surface amplification spectra are not much significant. However, such an exact conclusion does not arrive in case of deep deposits soil profiles. Based on overall analysis, it can be suggested for
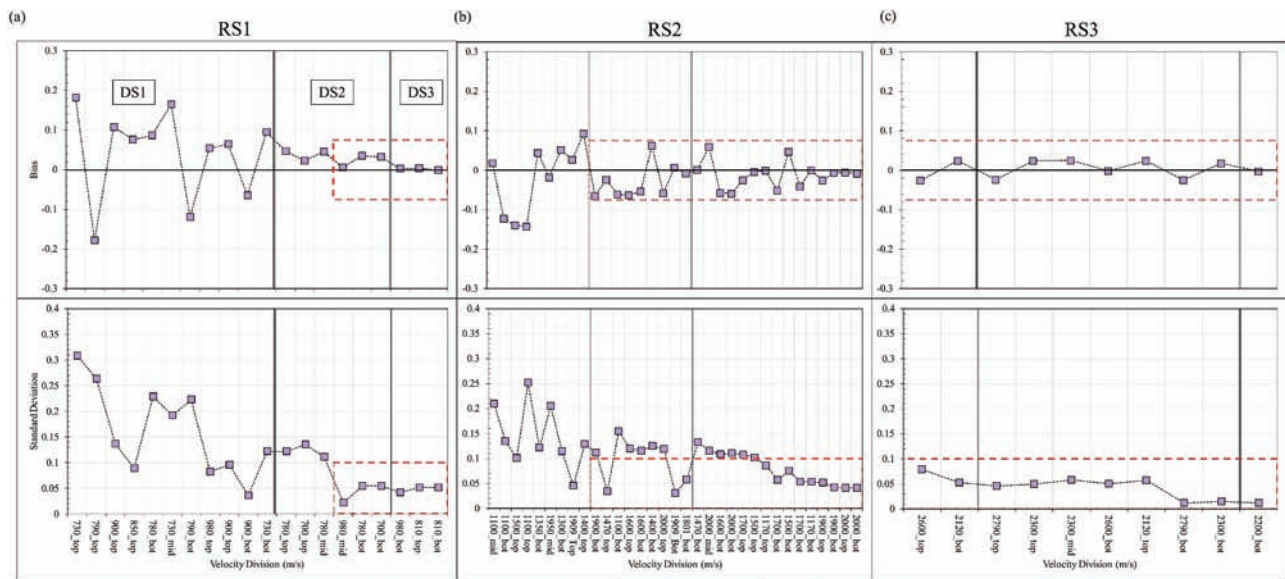
Figure 9. Variation of bias and standard deviation for the region (a) RS1, (b) RS2 and (c) RS3 for different velocity division for shallow sites. Thick vertical lines show the regions (DS1, DS2 and DS3) variability of these parameters for different depth division. Dashed box shows the region of less bias and standard deviation.

capturing the proper amplification factor at the surface; ground motion can be inputted at the layer having V_s equal to or more than 1200 m/s and above for shallow soil sites irrespective of depths. It can also be noted here that Anbazhagan *et al.* (2013) have observed no significant difference in response spectra at the surface when input motion at bedrock when V_s is between 1385 to 1868 m/s for shallow sites. The result in this study is almost similar to the previous study, which is based on hypothetical profiles.

8. Applicability and assumption of current study

In this study, a non-linear 1D site response model is considered for determining the depth of input motion. In the absence of grain size distribution, a qualitative estimate is used for soil classification into four broader categories rock, gravel, sand and clay. Based on Thompson *et al.* (2012), sites are selected for determining the poor and good fit for 1D wave propagation assumption, i.e. LP and LG sites. For LP sites, the vertical incidence is not presumed as a source of error. The difference in small strain damping ratio and shear wave velocity is used in attributing this error. Using the Monte Carlo simulations and linear 1D site response analysis, shear wave velocity profiles are estimated and used further in the analysis. 1D site response model that assumes horizontally polarised shear wave propagation assuming vertical incidence is used for analysis. Due to the lack of nonlinear material data and pore-pressure data for KiK-net sites, complicated non-linear constitute models could not be used. Depth of input motion derived in this study is not applicable for the sites where bottom most layer shear wave velocity is less than 700 m/s, especially in the case of deep sites deposits. For these sites, proper care needs to be taken for deriving the surface amplification using 1D non-linear site response analysis. Further, suppose in case a layer in between has more shear wave velocity than bottommost layer velocity. In that case, the input is suggested to be given at the bottommost layer only to capture the proper site surface spectra. Additionally, it is noted that these depths of inputting the motion can only be used as an initial estimate to predict the surface amplification spectra for the sites where information about bedrock is not available.

9. Conclusions

This study aims to identify the impact of input ground motion at different velocity layers on amplification and response spectrum and identify a suitable input layer for

shallow and deep bedrock sites using KiK-Net downhole array network data. Initially, all input parameters are calibrated by giving input at recorded depth, and exact matching input parameters (Vs, density and shear modulus and damping curves) are frozen for depth analysis. Using the mixed effect models on the residual calculated from recorded and predicted surface amplification spectra. Based on the obtained, fixed effect bias and standard deviation, representing velocity layer and depth, were selected.

- The study suggested that for capturing the proper amplification factor at the surface; ground motion can be inputted at the layer having V_s equal to or more than 1500 m/s for deep soil sites irrespective of depths.
- In many deep soil sites, layer with 1500 m/s may not be found within 200 m; in that case, ground motion can be inputted either at a layer having a velocity of 1000 m/s and above at a depth of 170 m and above for determining the reliable surface response values.
- Study found that site with low velocity (e.g. 730 m/s) at different depths, response spectra are over-predictive at a depth less than 30 m in case of deeper deposits. Bias and standard deviation for velocity and depth more than 1500 (−100) m/s and 100 (−15) m, the effect of inputting motion of surface amplification spectra are not much significant in the shallow sites. However, such an exact conclusion does not arrive in the case of deep deposits soil profiles.
- For capturing the proper amplification factor at the surface, ground motion can be inputted at the layer having V_s equal to or more than 1200 m/s and above for shallow soil sites irrespective of depths.

Disclosure statement

No potential conflict of interest was reported by the author(s).

Funding

ORCID

P Anbazhagan http://orcid.org/0000-0001-9804-5423

References

Abdullah, H.H., Fattah, M.Y., and Abed, A.H., 2018. Determination of liquefaction potential for two selected sites in Kerbala City- Middle of Iraq. *International Journal of Engineering & Technology*, 7 (1), 25–32. doi:10.14419/ijet.v7i1.8268.

Akin, M.K., Kramer, S.L., and Topal, T., 2016. Dynamic soil characterization and site response estimation for Erbaa, Tokat (Turkey). *Nat Hazards*, 82 (3), 1833–1868. doi:10.1007/s11069-016-2274-4.

Al–Damluji, O. F., Al–Shakarch, Y. J., and Fattah, M. Y. A. 2002. Coupled Dynamic Response Analysis of a Sand Layer to Earthquake Motion Using the Finite Element Method. *Journal of Engineering*, College of Engineering, University of Baghdad, 8(2), 213–231.

Anbazhagan, P., *et al.*, 2016. Correlation of densities with shear wave velocities and SPT N values. *Journal of Geophysics and Engineering*, 13 (3), 320. doi:10.1088/1742-2132/13/3/320.

Anbazhagan, P., *et al.*, 2017. Selection of representative shear modulus reduction and damping curves for rock, gravel and sand sites from the KiK-Net downhole array. *Nat Hazards*, 88 (3), 1741. doi:10.1007/s11069-017-2944-x.

Anbazhagan, P., Sheikh, M.N., and Parihar, A., 2013. Influence of rock depth on seismic site classification for Shallow Bedrock regions. *Natural Hazard Review ASCE*, 14 (2), 108–121. doi:10.1061/(ASCE)NH.1527-6996.0000088.

Anbazhagan, P. and Sitharam, T.G., 2008. Seismic microzonation of Bangalore. *Journal of Earth System Science*, 117 (S2), 833–852. doi:10.1007/s12040-008-0071-5.

Ansal, A. and Tonuk, G., 2007. Source and site factors in microzonation. *In*: K.D. Pitilakis, ed. *Earthquake geotechnical engineering, 4th international conference on earthquake geotechnical engineering-invited lectures*, Thessaloniki, Greece, 73–92.

Bajaj, K. and Anbazhagan, P., 2018. Determination of GMPE functional form for an active region with limited strong motion data: application to the Himalayan region. *Journal of Seismology*, 22 (1), 161–185. doi:10.1007/s10950-017-9698-5.

Bajaj, K. and Anbazhagan, P., 2020. Identification of shear modulus reduction and damping curve for deep and shallow sites: KiK-Net data. *Journal of Earthquake Engineering*, Published Online doi:10.1080/13632469.2019.1643807.

Bakir, B.S., Sucuoğlu, H., and Yilmaz, T., 2002. An overview of local site effects and the associated building damage in Adapazari during the 17 August 1999 Izmit earthquake. *Bulletin of the Seismological Society of America*, 92 (1), 509–526. doi:10.1785/0120000819.

Barani, S., Ferrari, R.D., and Ferretti, G., 2013. Influence of soil modeling uncertainties on site response. *Earthquake Spectra*, 29 (3), 705–732. doi:10.1193/1.4000159.

Boore, D.M. and Bommer, J.J., 2005. Processing of strong-motion accelerograms: needs, options and consequences. *Soil Dynamics and Earthquake Engineering*, 25 (2), 93–115. doi:10.1016/j.soildyn.2004.10.007.

Bradley, B.A., 2011. A framework for validation of seismic response analyses using seismometer array recordings. *Soil Dynamics and Earthquake Engineering*, 31 (3), 512–520. doi:10.1016/j.soildyn.2010.11.008.

Bradley, B.A. and Cubrinovski, M., 2011. Near-source strong ground motions observed in the 22 February 2011 Christchurch earthquake. *Seismological Research Letters*, 82 (6), 853–865. doi:10.1785/gssrl.82.6.853.

Chapman, M.C. and Talwani, P., 2002. Seismic hazard mapping for bridge and highway design, report to the South Carolina department of transportation, Columbia, SC.

Cramer, H., 2006. Quantifying the uncertainty in site amplification modeling and its effects on site-specific seismic-hazard estimation in the upper Mississippi embayment and adjacent areas. *Bulletin of the Seismological Society of America*, 96 (6), 2008–2020. doi:10.1785/0120060037.

Darendeli, M.B., 2001. Development of a new family of normalized modulus reduction and material damping curves. Ph.D. dissertation. University of Texas at Austin, Austin, Texas.

Dawood, H.M., *et al.*, 2016. A flatfile for the KiK-net database processed using an automated protocol. *Earthquake Spectra*, 32 (2), 1281–1302. doi:10.1193/071214eqs106.

Electric Power Research Institute (EPRI). 1993. Guidelines for Site specific ground motions, Palo Alto, California, November, TR-102293.

Fattah, M.Y., Abdullah, H.H., and Abed, A.H., 2018. Ground response analysis for two selected sites in Al-Hilla City in the middle of Iraq. *Journal of the University of Babylon for Engineering Sciences*, 26 (6), 235–257.

Gardner, G.H.F., Gardner, L.W., and Gregory, A.R., 1974. Formation velocity and density—the diagnostic basics for stratigraphic traps. *Geophysics*, 39 (6), 770–780. doi:10.1190/1.1440465.

Govindaraju, L. and Bhattacharya, S., 2012. Site-specific earthquake response study for hazard assessment in Kolkata city, India. *Natural Hazards*, 61 (3), 943–965. doi:10.1007/s11069-011-9940-3.

Grelle, G. and Guadagno, F.M., 2009. Seismic refraction methodology for groundwater level determination: water seismic index. *Journal of Applied Geophysics*, 68 (3), 301–320. doi:10.1016/j.jappgeo.2009.02.001.

Hashash, Y.M.A., *et al.*, 2008. Soil-Column depth-dependent seismic site coefficients and hazard maps for the Upper Mississippi embayment. *Bulletin of the Seismological Society of America*, 98 (4), 2004–2021. doi:10.1785/0120060174.

Hashash, Y.M.A., *et al.*, 2017. *DEEPSOIL 7.0.5, user manual*. Urbana: Board of Trustees of University of Illinois at Urbana-Champaign.

Hashash, Y.M.A. and Park, D., 2001. Non-linear one-dimensional seismic ground motion propagation in the Mississippi embayment. *Engineering Geology*, 62 (1–3), 185–206. doi:10.1016/S0013-7952(01)00061-8.

Hough, S.E., *et al.*, 2011. Site characterization and site response in Port-Au Prince, Haiti. *Earthquake Spectra*, 27 (1_suppl1), 137–155. doi:10.1193/1.3637947.

Inazaki, T., 2006. Relationship between S-wave velocities and geotechnical properties of alluvial sediments. *In*: *Proceedings of 19th annual symposium on application of geophysics to engineering and environmental problems (SAGEEP2006)*, 2-6 April, Seattle, Washington, USA, 1296–1303.

Ishibashi, I. and Zhang, X., 1993. Unified dynamic shear moduli and damping ratios of sand and clay. *Soils and Foundations*, 33 (1), 182–191. doi:10.3208/sandf1972.33.182.

Kaklamanos, J., *et al.*, 2013. Critical parameters affecting bias and variability in site response analyses using KiK-net downhole array data. *Bulletin of the Seismological Society of America*, 103 (3), 1733–1749. doi:10.1785/0120120166.

Kaklamanos, J., *et al.*, 2015. Comparison of 1D linear, equivalent-linear, and nonlinear site response models at six KiK-net validation sites. *Soil Dynamics and Earthquake Engineering*, 69, 207–219. doi:10.1016/j.soildyn.2014.10.016

Kumar, A., Anbazhagan, P., and Sitharam, T.G., 2012. Site specific ground response study of deep Indo-Gangetic basin using representative regional ground motion. Geo-Congress, State of art and practice in Geotechnical Engineering, Oakland California, Paper No. 1065, 1888–1897

Kwok, A.O.L., Stewart, J.P., and Hashash, Y.M.A., 2008. Nonlinear ground response analysis of Turkey Flat shallow stiff-soil site to strong ground motion. *Bulletin of the Seismological Society of America*, 98 (1), 331–343. doi:10.1785/0120070009.

Mahajan, A.K., *et al.*, 2007. Methodology for site response studies using multi-channel analysis of surface wave technique in Dehradun city. *Current Science*, 92 (7), 945–955.

Malekmohammadi, M. and Pezeshk, S., 2015. Ground motion site amplification factors for sites located within the Mississippi embayment with consideration of deep soil deposits. *Earthquake Spectra*, 31 (2), 699–722. doi:10.1193/091712EQS291M.

Menq, F.Y., 2003. Dynamic properties of sandy and gravelly soils. Ph.D. thesis. Department of Civil Engineering, University of Texas, Austin, TX.

Omar, M., *et al.*, 2013. Influence of local soil conditions on ground response: site amplification in Sharjah, United Arab Emirates. *International Journal of Modern Engineering*, 13 (2) Spring/Summer pp. 34–40, USA, .

Park, D. and Hashash, Y.M.A., 2005. Evaluation of seismic site factors in the Mississippi embayment—Part II: probabilistic seismic hazard analysis with nonlinear site effects. *Soil Dynamics and Earthquake Engineering*, 25 (2), 145–156. doi:10.1016/j.soildyn.2004.10.003.

Park, D., Pezeshk, S., and Hashash, Y., 2004. Nonlinear site response of deep deposits in West Tennessee, *In*: *Proceedings, 4th National Seismic Conference and Workshop on Bridges and Highways*, 9–12 February, Memphis, TN.

Pinheiro, J.C. and Bates, D.M., 2000. *Mixed-Effects models in S and S-PLUS*. New York: Springer-Verlag, 528.

Rollins, K., Evans, M., and Diehl, N.W., 1998. Shear modulus and damping relationships for gravels. *Journal of Geotechnical and Geoenvironmental Engineering*, 124 (5), 396–405. doi:10.1061/(ASCE)1090-0241(1998)124:5(396).

Seed, H., *et al.*, 1986. Moduli and damping factors for dynamic analyses of cohesionless soils. *Journal of Geotechnical Engineering*, 112 (11), 1016–1032. doi:10.1061/(ASCE)0733-9410(1986)112:11(1016).

Seed, H.B. and Idriss, I.M., 1970. Soil moduli and damping factors for dynamic response analyses. Technical Report EERRC-70-10, University of California, Berkeley.

Silva, W., 2008. Site response simulations for the PEER-NGA project, report prepared for the Pacific Earthquake Engineering Research Center.

Thompson, E.M., *et al.*, 2012. A taxonomy of site response complexity. *Soil Dynamics and Earthquake Engineering*, 41, 32–43. doi:10.1016/j.soildyn.2012.04.005

Vucetic, M. and Dobry, R., 1991. Effect of soil plasticity on cyclic response. *Journal of Geotechnical Engineering*, 117 (1), 89 107. doi:10.1061/(ASCE)0733-9410(1991)117:1(89).

Yang, Z., Yuan , J., Liu, J., Han, B. , *et al.*, 2017. Shear modulus degradation curves of gravelly and clayey soils based on KiK-Net In Situ seismic observations. Journal of Geotechnical and Geoenvironmental Engineering, 143 (9), 06017008.

Zhang, J., Andrus, R., and Juang, C.H., 2005. Normalized shear modulus and material damping ratio relationships. *Journal of Geotechnical and Geoenvironmental Engineering*, 131 (4), 453–464. doi:10.1061/(ASCE)1090-0241(2005)131:4(453).